

PV GROUND-FAULT DETECTION USING SPREAD SPECTRUM TIME DOMAIN REFLECTOMETRY (SSTDR)

Mohammed Khorshed Alam, Faisal Khan
 Power Engineering and Automation Research Lab (PEARL)
 Dept. of Electrical and Computer Engineering,
 University of Utah, Salt Lake City, Utah, USA
 Email: khorshed.alam@utah.edu

Jay Johnson and Jack Flicker
 Sandia National Laboratories, Albuquerque, NM, USA

Abstract— A PV ground-fault detection technique using spread spectrum time domain reflectometry (SSTDR) method has been introduced in this paper. SSTDR is a reflectometry method that has been commercially used for detecting aircraft wire faults. Unlike other fault detection schemes for a PV system, ground fault detection using SSTDR does not depend on the amplitude of fault-current and highly immune to noise signals. Therefore, SSTDR can be used in the absence of the solar irradiation as well. The proposed PV ground fault detection technique has been tested in a real-world PV system and it has been observed that PV ground fault can be detected confidently by comparing autocorrelation values generated using SSTDR. The difference in the autocorrelation peaks before and after a ground-fault in the PV system are significantly higher than the threshold set for ground-fault detection.

I. INTRODUCTION

Fault detection and isolation is an indispensable part of any electrical system. Failure to provide these protections may result in severe damage and downtime leading to economic loss, human injury or loss of life. Ground-faults are one type of most critical faults in PV systems, which result from

unintentional low-resistance path to the ground or earth. Many PV systems in the US “ground” one of the current-carrying conductors to provide a means of detecting ground faults with a ground-fault detection and interruption (GFDI) device. In general, GFDI is a fuse or a residual current circuit breaker (RCCB). This system prevents electrical shock and fire. However, the grounding practice and requirements depend on the application and varies between different countries. According to the US National Electrical Code (NEC), PV systems with system voltage more than 50V require a GFDI system [1]-[10]. A schematic diagram of a typical grounded PV system is shown in Fig. 1.

A ground-fault detection and interruption (GFDI) device is installed in a PV system to detect the ground-fault, and isolate the fault to protect the system from potential fire hazards. In general, ground-faults are detected if the fault current exceeds some predetermined value set by the GFDI devices. However, a GFDI system based on fault current measurement suffers from the following limitations:

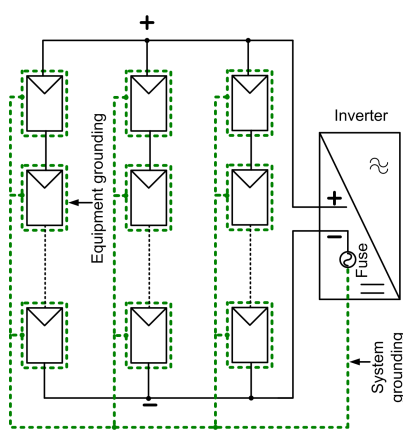


Fig. 1. PV system with proper grounding.

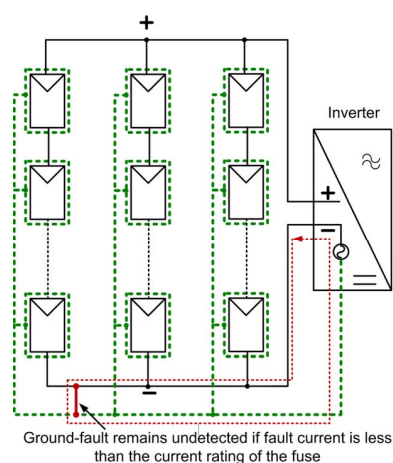


Fig. 2. A possible ground-fault in a PV system. This fault may/ may not be interrupted by the GFDI device.

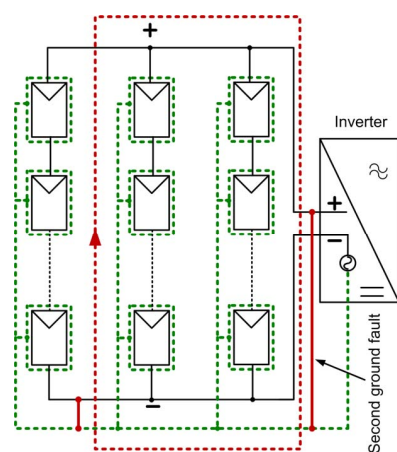


Fig. 3. Double ground-fault in a PV system. GFDI systems may fail to detect double ground fault as there is no circulating current flows through the fuse.

1) A ground-fault may occur in the absence of the solar irradiation (i.e., during night) and remain undetected [1] [5] [6].

2) Ground-fault current may be smaller than the GF DI threshold current limit [7] [8] and remain undetected. This is illustrated in Fig. 2.

3) GF DI based on differential current measurement may suffer from noise and provide misleading fault indication.

4) An undetected ground-fault may pose as a “normal condition” and allow formation of another ground-fault (double ground fault) [8]. This may establish a fault current path without any means of being interrupted by GF DI devices.

A possible double ground fault is shown in Fig. 3. Double ground-faults could be extremely dangerous for a PV system since the short circuit current may exceed 1300 A in a 500 kW PV array [8]. Both the PV system fires on April 5, 2009, in Bakersfield, California, and April 16, 2011, in Mount Holly, North Carolina are thought to be caused by double ground faults [7] [8]. Therefore, it is important to detect all ground faults to avoid any possible damage.

A new PV ground-fault detection technique based on spread spectrum time domain reflectometry is presented here. This method does not use traditional current/voltage measurement/sensors to detect ground faults. Therefore, this is free from the limitations of conventional ground fault detection techniques. SSTDR technique has been commercially used for detecting aircraft wire faults, and it has the potential to detect short-circuit or open-circuit fault even

in an energized system [18] [19].

II. SPREAD SPECTRUM TIME DOMAIN REFLECTOMETRY (SSTDR)

Reflectometry is an electrical characterization technique based on the reflection of the incident signal through a transmission line. Reflection of an electrical signal is one important property of transmission lines. Whenever the length of the transmission line is comparable to the wavelength of the transmitted signal, there exist reflections of the signal at any impedance discontinuity. A simple transmission line of characteristic impedance Z_0 and length L connected to a load impedance Z_L is shown in Fig. 4. A voltage signal (V^+) applied at $x=-L$ will travel through the length of the transmission line and a voltage signal (V^-) will reflect back from the point of discontinuity at $x=0$. The ratio of reflected signal in proportion to the incident signal depends on the characteristic impedance of the transmission line and the load impedance connected at the end point of the line. The reflection coefficient (ρ) is defined as the ratio of the incident voltage signal to the reflected voltage signal at the load terminal, and can be calculated using equation (1) [11].

$$\rho = \frac{V^+}{V^-} = \frac{Z_L - Z_0}{Z_L + Z_0} \quad (1)$$

Different types of reflectometry methods have been widely used for wire fault detection and impedance measurement. A comparison among different reflectometry methods has been discussed in [12]-[17]. In spread spectrum

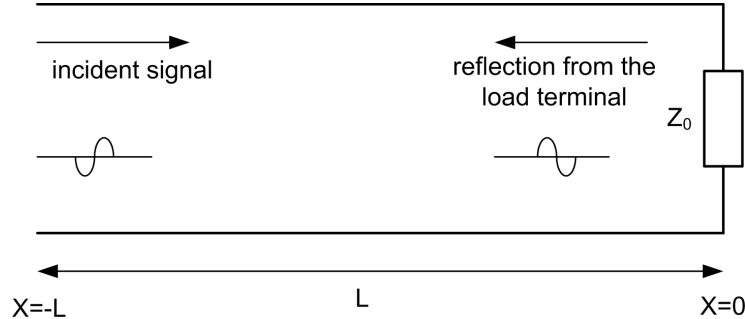


Fig. 4. Simplified schematic diagram of a transmission line.

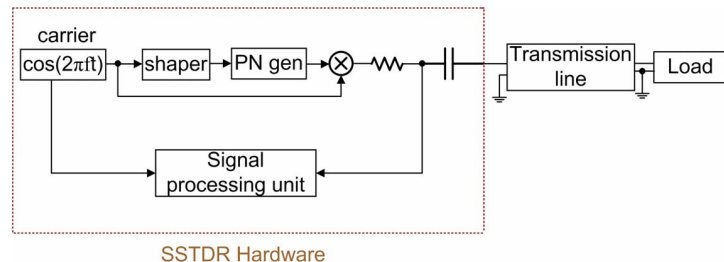


Fig. 5. Block diagram of SSTDR test system [13].

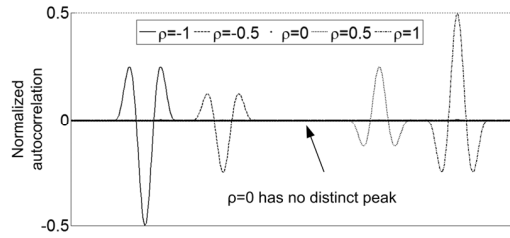


Fig. 6. Variation in normalized autocorrelation peak for different values of reflection co-efficient.

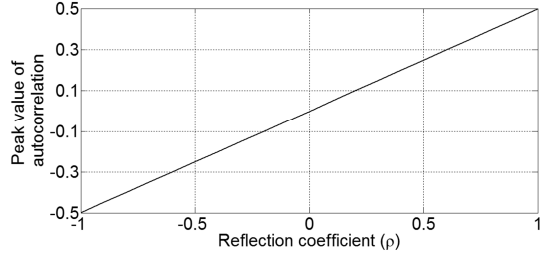


Fig. 7. Variation in normalized autocorrelation peak for different values of reflection co-efficient.

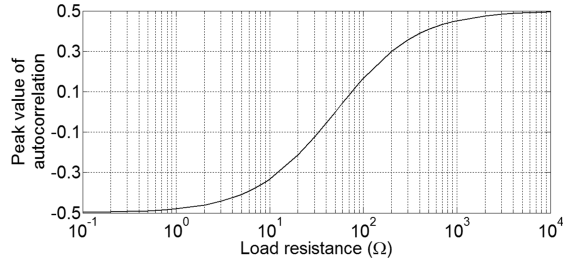


Fig. 8. Variation in normalized autocorrelation peak vs. load resistance connected at the end of a $75\ \Omega$ transmission line.

time domain reflectometry, a binary pseudo-noise (PN) code modulated sinusoidal wave is sent through a transmission wire and an autocorrelation of the incident wave with the reflected wave provides information on the length of the transmission line and the impedance of the load connected at the end point of the transmission line.

SSTDR is superior to other reflectometry techniques because of lower cost and higher noise immunity compared to other reflectometry methods. A block diagram of the SSTDR system is shown in Fig. 5. Normalized autocorrelation curves for different values of ρ have been generated in MATLAB and shown in Fig. 6. These autocorrelation curves have been generated with arbitrary delays for better presentation. The shape of the lobes at the point of discontinuity does not change for any change in reflection coefficient. However, the peak value of the main lobe changes with a change in the reflection coefficient. $\rho = -1$ represents a short circuited transmission line, $\rho = +1$ represents an open circuited



(a)



(b)

Fig. 9. Facilities used at DTEL at Sandia National Lab to perform the tests.

transmission line and $\rho=0$ represents a characteristic impedance matched transmission line.

In these experiments, the same signal is sent through the transmission line resulting in a linear relationship between the autocorrelation peak value and the reflection coefficient (Fig. 7). However, the relationship between the reflection coefficient and the load impedance is related by equation (1). Therefore, the relationship between the load resistance and the reflection coefficient/ autocorrelation peak is not linear. A plot has been generated in MATLAB showing the relationship between the impedance of a resistive load connected at the end of a $75\ \Omega$ transmission line and the corresponding normalized autocorrelation peak (Fig. 8). The peak of the autocorrelation function always increases with an increase in load resistance and any variation in the autocorrelation peak has a direct relationship with variation in load or characteristic impedance.

Any ground fault in a PV system introduces significant local impedance variation compared to a healthy PV system (system without ground fault), and the proposed SSTDR scheme can detect the ground fault by comparing the autocorrelation values of the PV system before and after the fault occurred.

III. PV GROUND FAULT DETECTION USING SSTDR

The proposed ground fault detection technique has been implemented at the Distributed Energy Technologies Laboratory (DETL) of Sandia National Laboratories (SNL) shown in Fig. 9. A WILMA LWG40414 hardwire device (based on SSTDR technology from Livewire Innovation) [18] has been used to interface with a de-energized PV system to generate the autocorrelation values. Specifications of each PV module are shown in Table 1.

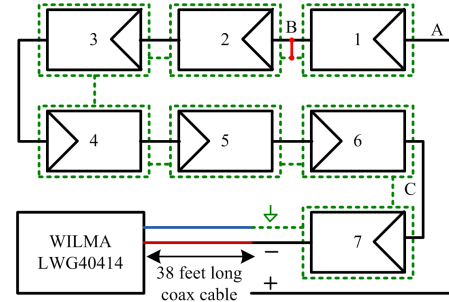
Seven PV modules were connected in series and SSTDR hardware was connected to the negative and ground terminals of the PV system through a ~38 foot long RG-59/U coaxial cable of characteristic impedance 75Ω . A schematic diagram of the test setup and photograph of the WILMA LWG40414 board are shown in Fig. 10. A PV ground fault was created by connecting the positive or negative terminal of any PV module to the ground wire of the PV system through a fuse having $0.5\ \Omega$ internal resistance. Fig. 10(a) illustrates a ground fault at location B. The WILMA LWG40414 can generate SSTDR signals with carrier frequencies from 375 kHz to 96 MHz (refer to Fig. 5). The distance resolution of the autocorrelation increases and the range decreases with an increase in carrier frequency. A carrier frequency of 48 MHz was selected as it provides the best range and resolution for this test setup.

Each test was performed ten times, and the results were averaged to minimize the inherent noise of the SSTDR hardware. Ten autocorrelation plots along with the average for a healthy PV system are shown in Fig. 11. There are two distinguishable peaks in the autocorrelation curve for a healthy PV system. The first peak is due to the impedance mismatch between the SSTDR output terminal and the coaxial cable, and the second peak is at the interface of the coax cable and PV wires. The variation in the ten sets of autocorrelation values is low at the peaks of autocorrelation plot, and these peaks indicate impedance mismatches along the transmission line. In order to create an alarm threshold for the SSTDR ground fault detector, the variability in the healthy system was investigated. The measurement noise was determined to be less than 400, so a conservative threshold was set at 1000. This prevents nuisance tripping while still capturing the different ground faults.

Three separate PV ground faults were created at different locations marked as A, B, C in Fig. 10. Ten sets of autocorrelation data were collected and averaged for each ground fault. The average autocorrelation response for a healthy PV system and a system with ground fault are shown in Fig. 13, and the autocorrelation response of a healthy PV system was distinguishable from a PV system with a ground fault. In order to demonstrate this, the area from 35 feet to 100 feet in Fig. 13 is shown in Fig. 14. Differences between the autocorrelation values for PV systems with a ground fault and a healthy PV system are shown in Fig. 15. This difference can be as high as 9000 irrespective of the location of the

Table 1. Specification of a PV module used in the test setup (at $1000\text{W/m}^2, 25^\circ\text{C}$ cell temperature)

Maximum power (P_{\max})	200W
Short circuit current (I_{sc})	3.83 A
Open circuit voltage (V_{oc})	68.7 V
Maximum power current (I_{pmax})	3.59 A
Maximum power voltage (V_{pmax})	55.8 V



(a)



(b)

Fig. 10. (a) Schematic of the test setup showing fault at location B only, (b) WILMA LWG40414.

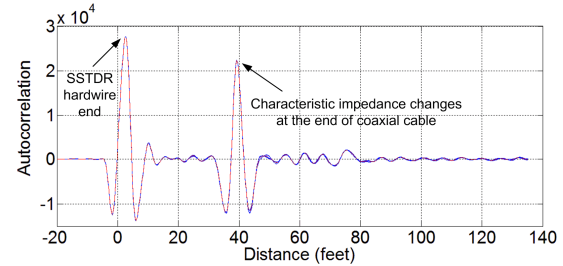


Fig. 11. Autocorrelation data (10 sets-blue lines) are plotted with average autocorrelation data (red line) vs. distance.

ground fault and is much higher than the threshold for fault detection (1000). Fig 16 shows a magnification of the autocorrelation data between 38 feet and 40 feet to illustrate the difference in values for ground fault in different locations (A, B, or C).

Ground faults at different locations generate an autocorrelation plot that is distinct from the autocorrelation plot for a healthy PV system and provides insight into the location of the fault. However, metal conductors, frames of the PV modules, and solar cells itself introduces complex distributed capacitances and other parasitic components between the current carrying conductors and ground [20]. Therefore, extensive research on frequency dependent parameterization of the PV system is necessary along with insight into the complex data processing needed to locate ground fault position after a fault has been detected.

IV. CONCLUSIONS

Traditional ground-fault detection and interruption (GFDI) devices rely on current sensors/measurement devices. PV ground-fault current might be below the threshold current value of the GFDI. Therefore, there is a chance that the ground fault might remain undetected. This may lead to a second ground fault which can cause a fire. A PV ground fault detection technique using spread spectrum time domain reflectometry method has been introduced in this paper. This technique is based on the impedance variation in a PV system due to the ground fault and does not depend on the amplitude of the fault current. Therefore, this method can be used in absence of the solar irradiance as well. This proposed technique for detecting ground faults in a PV system has been tested on a real-world PV string consisting of seven series connected PV modules. Ground faults introduced in the string resulted in a variation in the autocorrelation plot generated by the SSTDR hardware. Variation in autocorrelation peaks are significantly higher than the threshold set for ground fault detection.

V. ACKNOWLEDGEMENT

The authors express their appreciation to the US Department of Energy Office of Energy Efficiency and Renewable Energy for supporting this work, and Prof. Cynthia Furse of University of Utah for suggestions concerning the research.

REFERENCES

- [1] Y. Zhao, J. de Palma, J. Mosesian, R. Lyons, B. Lehman, "Line-Line Fault Analysis and Protection Challenges in Solar Photovoltaic Arrays," IEEE Transactions on Industrial Electronics, vol.PP, no.99, pp.1.
- [2] National Electrical Code, Article 690 - Solar Photovoltaic Systems, 2011.
- [3] IEA, "Utility aspects of grid connected photovoltaic power systems," IEA, Rep. IEA-PVPS T5-01:1998, 1998.
- [4] J. Wiles, "Photovoltaic Power Systems and the 2005 National Electrical Code: Suggested Practices," Southwest Technology Development Institute, Rep. Electronic version 1.91, 2010.
- [5] Ye Zhao, B. Lehman, J. de Palma, J. Mosesian, R. Lyons, "Challenges to overcurrent protection devices under line-line faults in solar

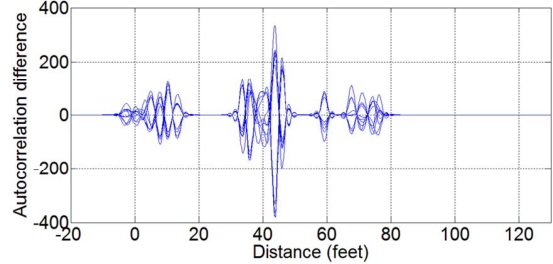


Fig. 12. Difference between the autocorrelation data (10 sets) and its average for a healthy PV system.

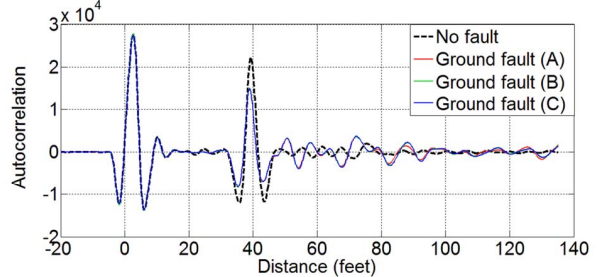


Fig. 13. Autocorrelation data for the healthy PV system (dashed black line) with autocorrelation data for PV system with ground fault at different locations

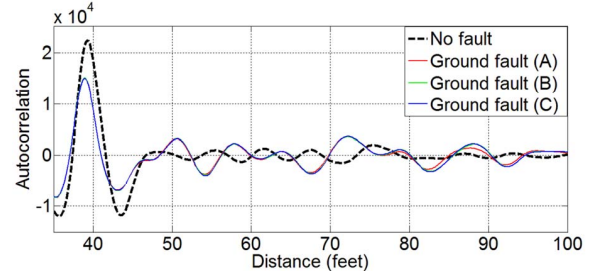


Fig. 14. Enlarged version of Fig. 13 (from 35 feet to 100 feet).

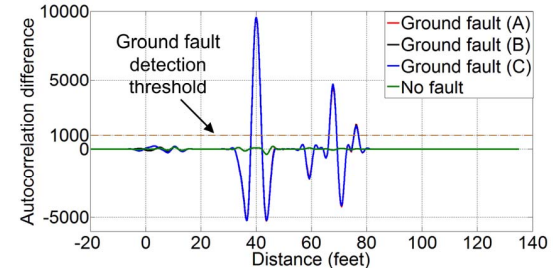


Fig. 15. Difference between autocorrelation data for the healthy PV system with autocorrelation data for PV system with ground fault.

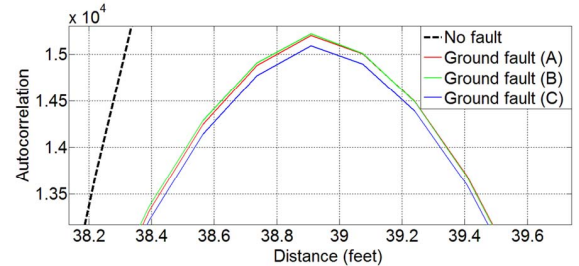


Fig. 16. Enlarged version of Fig. 14 (from 38 feet to 40 feet).

- photovoltaic arrays," 2011 IEEE Energy Conversion Congress and Exposition (ECCE), pp.20-27.
- [6] Y. Zhao, B. Lehman, J.F. de Palma, J. Mosesian, and R. Lyons, "Fault evolution in photovoltaic array during night-to-day transition," in Proc. IEEE COMPEL, 2010, pp. 1-6.
 - [7] Bill Brooks, "The Ground-Fault Protection BLIND SPOT: A Safety Concern for Larger Photovoltaic Systems in the United States", A Solar ABCs White Paper, January 2012, pp. 1-10.
 - [8] B. Brooks, " The Bakersfield Fire - A Lesson in Ground-Fault Protection", SolarPro Mag., 2011, pp. 62-70.
 - [9] H. Braun, S. T. Buddha, V. Krishnan, A. Spanias, C. Tepedelenlioglu, T. Yeider, and T. Takehara, "Signal Processing for Fault Detection in Photovoltaic Arrays" IEEE International Conference on Emerging Signal Processing Applications (ESPA), 2012 , pp. 115-118.
 - [10] W. Bower, J. Wiles, "Investigation of Ground-fault Protection Devices for Photovoltaic Power System Applications", Twenty-Eighth IEEE Photovoltaic Specialists Conference, 2000, pp. 1378-1383.
 - [11] F. T. Ulaby, "Fundamentals of applied electromagnetics", New Jersey: Prentice Hall, 2001, chapter 2.
 - [12] C. Furse, Y. C. Chung, C. Lo, P. Pendayala, "A Critical Comparison of Reflectometry Methods for Location of Wiring Faults"; Smart Structures and Systems, vol 2, Issue 1, pp. 25-46, 2006.
 - [13] P. Smith, C. Furse, J. Gunther "Analysis of spread spectrum time domain reflectometry for wire fault location", IEEE Sensors Journal, Vol. 5, Issue 6, December 2005, pp 1469 -1478.
 - [14] Chet Lo, C. Furse, "Noise Domain Reflectometry for Locating Wiring Faults", IEEE Transactions on Electromagnetic Compatibility, vol. 47, no. 1, pp. 97-104, February 2005.
 - [15] Tsai, P., Chet Lo, You Chung Chung, Furse, C., "Mixed-signal reflectometer for location of faults on aging wiring"; Sensors Journal, IEEE, vol 5, Issue 6, pp. 1479-1482, December 2005.
 - [16] Huibin Zhu, Allen R. Hefner, and Jih-Sheng Lai, "Characterization of power electronics system interconnect parasitic using time domain reflectometry", IEEE Trans On Power Elec, vol 14, n 4, july 1999.
 - [17] Daeil Kwon, Michael H. Azarian, and Michael Pecht; "Non-Destructive Sensing of Interconnect Failure Mechanisms Using Time Domain Reflectometry"; IEEE Sensors Journal, 2010.
 - [18] Livewire Innovation (<http://livewireinnovation.com>).
 - [19] P. Smith,C.Furse, J.Gunther, "Fault Location on Aircraft Wiring Using Spread Spectrum Time Domain Reflectometry", IEEE Sensors Journal, Vol.5, No. 6, Dec. 2005, pp. 1469-1478.
 - [20] Clément Miquel. "Frequencies Studies Applied to Photovoltaic Modules", Master Thesis, Royal Institute of Technology, Stockholm, Sweden 2011.